JOURNAL OF CATALYSIS 33, 210–218 (1974)

Selected Properties and Electronic Spectra for a Series of Copper(II) Alkali, Alkaline Earth, and Lanthanide Metal Chloride Oxyhydrochlorination Catalysts on Alumina

RONALD L. DOTSON

Diamond Shamrock Corporation, T. R. Evans Research Center, Painesville, Ohio 44077

Received August 28, 1973

Some selected properties for a series of copper(II) oxyhydrochlorination (OHC) catalysts were determined. Copper(II) alkali, alkaline earth, and lanthanide metal chloride salts were supported on alumina in each case. The electronic spectral frequencies, crystal field band shapes, and band assignments were used to define and correlate some of the microscopic and macroscopic characteristics of these systems. The overall fluidization properties are hereby related to substructure in each matrix. After a thermal cycling to 300°C for 24 hr, the electronic spectra and X-ray powder diffraction patterns run at 25°C, provide evidence for the existence of two separate and distinctly different anionic defect site symmetries about copper(II). In the presence of K^+ and Cs^+ ions a pseudotetrahedral, D_{2d}, $CuCl_4^{2-}$ ion is observed and with Mg^{2+}, La^{3+}, and Li^+ ions, a tetragonally distorted O_h, $CuCl_6^{4-}$, ion is found. The D_{2d} system has been reported to have much better fluidization properties and subsequently improved reaction rates because of better particle size distribution during OHC operation.

Introduction

For a number of years, halogenated hydrocarbons have been formed industrially using the reaction of an olefin, such as ethylene, propylene, or butylene, in a homogeneous or heterogeneous catalyst system. The catalysts are normally made to include a transition metal halide that has a variable valence. During the process the metal is reduced to a lower valence state, thereby producing chlorine atoms during the electron transfer step, which readily attack and saturate the olefinic double bonds. The reduced metal chloride is subsequently returned to its former oxidation state by reactions with hydrogen chloride and an oxidizing gas such as air. The oxidation step can be affected either simultaneously along with olefin halogenation or immediately thereafter (*1*).

The specific hydrocarbon halogenation process under study here is referred to as oxyhydrochlorination (OHC), and is very important commercially, since it is one of the primary steps in the manufacture of vinyl chloride (VC). It is used directly for the production of ethylene dichloride (EDC), a precursor for VC. The monohalogenated olefins like VC are valuable commercial products because they are precursors for various polymeric materials with large volume sales (*1*).

The present work deals with the electronic spectra and X-ray diffraction studies that correlate and define some of the most important *in situ* fluidization and catalyst properties. In order to define the actual site symmetry of the copper(II) ions in each matrix, the crystal field spectra are compared with X-ray diffraction data on known compounds. This information is compared with tests of fluid bed catalysts carried out in small-scale lab reactors (*2*).

Experimental

Sample Preparation

For each sample, a neutral alumina support was impregnated with cupric chloride and the associated salts from aqueous solutions. The support was evacuated to 30 Torr for 20 min prior to its treatment, and then the solution was introduced into the support over a 3-min time period. After an added 2-min imbibition period, the vacuum was broken and the excess solution removed from the freshly impregnated support by vacuum filtration for 60 min. The fresh catalyst was then dried at 120°C for 16 hr. One 330-g quantity of the dried catalyst was tested for agglomeration resistance and activity and the remainder subsequently heated to 300°C in air for 24 hr and then stored under vacuum to be assayed with electronic reflectance spectroscopy and X-ray powder diffraction techniques.

All materials other than CsCl and $LaCl_3$ were reagent-grade as obtained from the Fisher Scientific Company. The CsCl was obtained at 99% purity levels from Alfa Products Division of Ventron Corporation, and the $LaCl_3$ at 99% purity levels from Research Organic-Inorganic Chemical Corporation. In every case, the concentration of the impregnating solution in distilled water was calculated and ~0.75-g equivalents of the second component per gram atom of copper(II). In the three-component catalyst, $LaCl_3$ was present at about 0.3-g equivalents per gram atom of copper(II) chloride.

The catalyst support in each case was Alcoa-grade A-1 neutral calcinated alumina with a reported surface area of 20–70 m^2/g.

Measurement Techniques

The electronic reflectance spectra were taken on a Beckman DK-2 Ratio Recording Spectrophotometer. Samples were transferred from a vacuum desiccator to the reflectance cells fitted with quartz windows sealed airtight with neoprene O-rings. In each case, magnesium carbonate was used for sample diluent and reference standard.

The X-ray powder diffraction patterns for these samples were recorded with a Philips Norelco diffractometer and associated equipment.

Many observations were made on full-scale pilot reactors, and the dynamic fluid bed testing in the lab was carried out in a 37-mm i.d. Pyrex reactor equipped with a glass frit distributor plate sealed into the bottom and having an axial thermowell. A winding of resistance wire was put around the outside surface of the vessel. The resistance wire winding was overlaid with fiberglass insulation. Two long diametrically opposed holes in the insulation were used to observe the fluid bed. Power for the resistance heater winding was controlled with a Honeywell Dial-A-Trol Model R7350A-1263 temperature indicator controller, actuated by signals from a chromel-alumel thermocouple set into the axial thermowell.

Olefin, hydrogen chloride, and air were metered into the entrance chamber of the reactor through calibrated rotometers, mixed, and fed without preheating through the distributor frit and into the reaction zone of the vessel. A total feed gas flow rate of 900 cc/min at 25°C and one atmosphere was used.

These Alcoa A-1 supported catalysts containing only $CuCl_2$ are very prone to agglomerate when they are exposed to excess HCl in the OHC reaction. The resistance to agglomeration was gauged from the reaction temperature that was required to produce a 2-in. layer of stagnant catalyst above the frit. Agglomeration was induced by proportioning the HCl and air feeds to hold a stoichiometric excess of oxygen and HCl at all test temperatures beginning at 300°C. Each catalyst was held at a given temperature for 2 hr while the fluidization was observed. After the initial study, the temperature was increased by 10°C, the feed ratio adjusted, and the procedure repeated on the exposed bed. This same test procedure was repeated several times on each catalyst. Between each set of tests the catalyst was screened and the Pyrex reaction vessel rinsed with dilute nitric acid.

Results and Discussion

Reactions

The oxidation state of copper in the OHC catalyst couple obviously cycles between Cu(II) and Cu(I). For the conversion of ethylene to EDC the reaction sequence is usually written in the following manner (*2*):

$$CH_2{=}CH_2 + 2CuCl_2 \rightleftharpoons ClCH_2CH_2Cl + 2CuCl \quad (1)$$

$$\tfrac{1}{2}O_2(g) + 2CuCl \rightleftharpoons CuOCuCl_2 \quad (2)$$

$$2HCl(g) + CuOCuCl_2 \rightleftharpoons 2CuCl_2 + H_2O \quad (3)$$

$$CH_2{=}CH_2 + 2HCl(g) + \tfrac{1}{2}O_2(g) \rightleftharpoons ClCH_2CH_2Cl + H_2O \quad (4)$$

Most of the copper on the support can be converted into one or the other of these oxidation states by varying the reactant ratios (*3*).

Spectra and Diffraction Patterns

In the spectrum of each catalyst system matrix, typical *d–d* electronic transitions of copper(II) appear as weak bands at long wave lengths. The spectral band shapes, frequencies, and intensities are functionally dependent upon ligand field geometry, ion polarizing ability, and ion–ion proximity as the partially filled *d*-electron subshell about the copper(II) nucleus in each case is perturbed within the catalyst matrix (*4*).

The X-ray diffraction patterns observed for the $CuCl_2$–CsCl–alumina catalyst system are characteristic of pure $CsCuCl_3$. All of the structural band assignments made from the electronic reflectance spectra, in this case, are confirmed by the X-ray data. The spectral band analysis of copper(II) under these conditions indicates a strong *d–d* combination band composed of 10,989 and 7,936.5 cm^{-1} components due to the $^2E \rightarrow {}^2B_1$ and $^2E \rightarrow {}^2A_1$ transitions, respectively, and indicating thereby a D_{2d} ligand polyhedron about Cu^{2+} within the catalyst matrix, as shown in Figs. 1 and 4 and Table 2 (*5, 6*).

The $KCuCl_3$ analog of the $CsCuCl_3$ double salt is not stable in moist air, so that its X-ray diffraction patterns were not observed. From previous X-ray studies, however, $KCuCl_3$ is known to have a NH_4CdCl_3 structure, which has been modified to give the copper ion four nearest neighbors. This concept is corroborated by the electronic reflectance spectroscopy studies that in Figs. 1–3, show very intense *d–d* combination bands at 11,428.5; 11,890 cm^{-1} and 9,706.8; 9,852.2 cm^{-1} due to the $^2B_2 \rightarrow {}^2A_1$ and $^2B_2 \rightarrow {}^2E_1$ transitions, re-

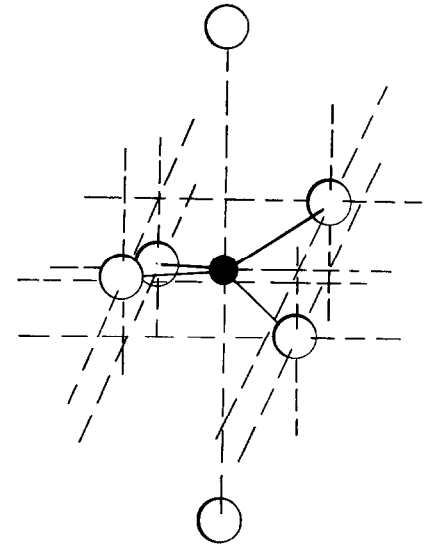

FIG. 1. Environmental site symmetry of the copper(II) ions in α-alumina impregnated with cesium(I) and potassum(I) ions. Where ○ represents Cl^- or O, and ● represents Cu^{2+} ions at the $CuCl_4^{2-}$ defect site.

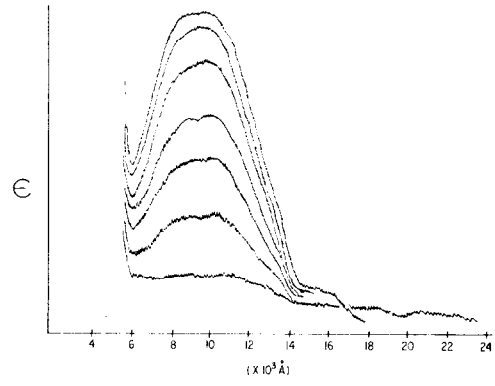

FIG. 2. Reflectance spectra of α-alumina containing 3.3% $CuCl_2$, 1.37% KCl, and 0.6% $LaCl_3$.

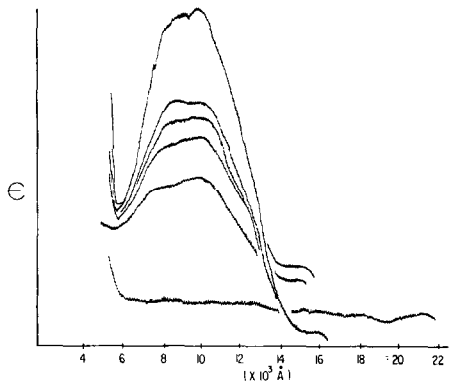

FIG. 3. Reflectance spectra of α-alumina containing 4% $CuCl_2$ and 1.67% KCl.

spectively, and again showing a D_{2d} ligand field about the Cu^{2+} point defects (*5*, *6*).

All of the other catalyst systems studied, e.g., $MgCl_2$–, $LaCl_3$–, and LiCl–$CuCl_2$–alumina, exhibited spectra typical of tetragonally distorted O_h symmetry fields, $\tilde{O}_h$, about the copper(II) ion as given in Figs. 5–8. In this case, the 10Dq band appears at the usual 12,903.2; 12,345.7; 12,980 cm^{-1} energies with a typical Jahn-Teller shoulder at 8,403.4; 8,058; 8,003 cm^{-1}, due commonly to the $^2T_{2g} \rightarrow {}^2E_g$ transitions (*7*).

Fluidization and Complex Ion Model

A qualitative explanation for the dramatic variation in symmetry about the copper(II) ion sites observed in going from K^+ and Cs^+ to Mg^{2+}, La^{3+}, and Li^+ chloride matrix salts can be given by assuming that a "complex-ion" model exists for the cupric chloride in the alumina matrix after the mixed salts of the catalyst have been exposed to molten salt conditions.

The structural data obtained relate to the fluidization tests, which showed that CsCl– and KCl–$CuCl_2$ systems in alumina were far superior to the others tested because of their improved fluidization and agglomeration resistance. Satisfactory fluidization conditions cannot be maintained with excesses of fine particles present because they tend to clump and agglomerate if moist or tacky. The solid particle size and size distribution thus are important factors in maintaining effective fluidization. This is commercially interesting, since at high temperatures the agglomeration and sintering of fine particles necessitates a lowering of the operating temperature and subsequently considerably reduced reaction rates (*8*).

In this case, the "complex-ion" is a submicroscopic structural entity used to describe the tendency toward stabilization, and the tendency towards stabilization of a component in solution is characterized by negative values of the chemical potential, μ. Some of the most important solution parameters influencing μ are: polarization effects, ligand field effects, coulomb interactions, packing and steric effects, and Van der Waal's interactions.

Since no self-consistent theory exists for defining and relating all of the above functions, the kinetic definition of "complex-ion" in terms of the lifetime of a grouping or of the relative ionic mobility, cannot be directly related to the equilibrium thermodynamic properties, such as μ, or to "complex-ions" as structural entities unless their lifetimes are very long.

Even when solids are heated near to their melting point, a limited amount of bulk flow occurs, because they behave like viscous materials with a strain rate that is proportional to the applied stress. Estimates of their surface tension can be made based on the change in the lattice parameters of small crystals. When a solid interface is destroyed, as in the case of dissolution, the excess surface-free energy appears as a delta heat of solution and the small differences between the heat of solution of course and finely crystalline materials can be measured with accurate calorimetry (*10*).

The halides of certain of the divalent metals like $CuCl_2$ can form anionic complexes having various symmetry forms when dissolved in molten alkali halide salt mixtures. The melting ranges for mixed catalyst salts are depressed, as opposed to pure $CuCl_2$ and CuCl, and fall between 260° and 460°C with 20 to 40 weight percent of potassium chloride (*11*).

The phase diagrams indicate that solu-

TABLE 1

RELATIVE ION POLARIZING STRENGTHS: $\frac{|Z|}{r^2}$

Ion	$\frac{\lvert Z\rvert}{r^2}$	Ionic radii r in Å	
		Pauling	Goldschmidt
O^{2-}	1.1	1.40	1.45
Cl^-	0.3 ←←	1.81	1.81
Li^+	1.7	0.68	0.60
K^+	0.6 ←←	1.33	1.33
Cs^+	0.4 ←←	1.67	1.69
Mg^{2+}	3.3	0.65	0.65
Al^{3+}	9.2	—	—
La^{3+}	2.0	1.15	1.04
Cu^+	0.5 ←←	0.96	0.95
Cu^{2+}	0.42←←	—	0.92

tions of up to 30 mole percent MCl_2* in KCl can be treated as ideal Temkin solutions of K^+ cations and Cl^- anions, and complex anions MCl_4^{2-} (*12*). In any case, the molten salt may be considered as a quasi-lattice. Combinations of alkali halides having a common ion, and showing their typical isomorphism, tend to provide continuous solid solutions when the relative differences in interionic distances are small enough.

Polarization and ligand field effects. As the type of alkali or alkaline earth cation, A^+,† is examined when moving up the periodic group from Cs^+ to Li^+, there is observed to be an increasing tendency for these pseudotetrahedral, MCl_4^{2-}, complexes to dissociate into Cu^{2+} and Cl^- ions. To a first-order approximation, the dissociative process occurs because of the progressive periodic changes in the relative ion-polarizing strengths and the resulting matrix relaxation, as given in Table 1. At the *isopolarization point* of the given ionic-covalent catalyst matrix, a discrete anion complex model is induced and then the MX_4^{2-} structure can remain almost static during and after the 300°C cooling cycle (*9, 13*). The MX_4^{2-} complexes tend to become much less stable as the A^+ ion changes from Cs^+ to Li^+. Since Cs^+ and K^+ are

* Where M can be any transition metal, and Cu^{2+} in this case.

† Where A is any alkali or alkaline earth metal.

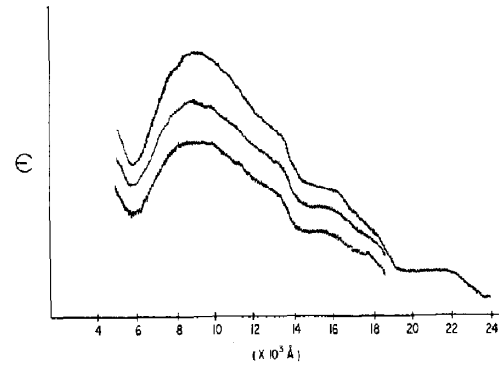

FIG. 4. Reflectance spectra of α-alumina containing 3.9% $CuCl_2$ and 4.1% CsCl.

nearly isopolar with Cl^-, the MX_4^{2-} rate of dissociation is much lower with these ions being present. A D_{2d} symmetry form then dominates on a time average basis for the Cu(II)–Cu(I) couple under these conditions. The principal forces involved with keeping the structure from becoming coplanar and D_{4h} or $\tilde{O}_h$ have been calculated. The results are shown by the structures in Fig. 1 and related spectra in Figs. 2–4.

The two important contributions to the energy in this system arise from electrostatic repulsion of the ligand point charges and the splitting of the 3*d* orbital energies of Cu^{2+} in the field of the point charges. The mutual repulsion of the point charges of Cl^- ions tends to stabilize the tetrahedral configuration relative to the square coplanar while the splitting of the 3*d* energy levels does the opposite, because the splitting becomes greater as the configuration goes from tetrahedral to coplanar. The total energy of the system can be minimized with respect to a spherical harmonic expansion of the 3*d* electron shell radius of copper to obtain bond angles 2Θ and 2γ with values 118.9° and 105° and thus agreeing well with experiment (*14*).

Table 1 and associated data indicate that in each case much more ordering is produced in a given matrix when the difference in polarizing power, proportional to $|Z|/r^2$, between two different cations increases, since a smaller cation prefers to be located near to a larger anion. With polarizing strengths greater than around

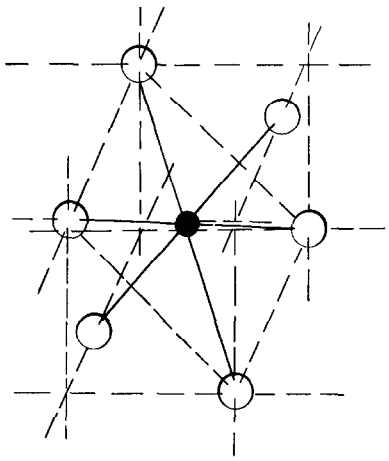

FIG. 5. Environmental site symmetry of the copper(II) ions in α-alumina impregnated with lithium(I), magnesium(II), and lanthanum(III) ions, respectively. Where ○ represents Cl^- or O, and ● represents Cu^{2+} ions at the $CuCl_6^{4-}$ defect site.

0.6, and with ions studied other than Cs^+ and K^+, the symmetry of the ligand field about the copper(II) ion couple indeed increases abruptly to a tetragonally distorted $\tilde{O}_h$ in the melt, since this is the most stable form for copper(II) commonly observed. The latter MCl_6^{4-} structure is shown in Fig. 5, and related spectra in Figs. 6–8 (*13, 15*).

Coulomb interaction. The long-range electrostatic interactions in the catalyst submonolayers operate at considerable distances, on the molecular scale, to activate

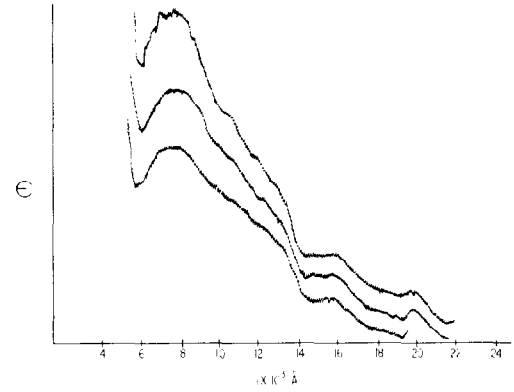

FIG. 7. Reflectance spectra of α-alumina containing 4.1% $CuCl_2$ and 1.86% $LaCl_3$.

certain short-range effects at the catalyst particle surface due mainly to the penetration of and polarization of the *d* subshells of copper(II), noted in Fig. 9, and Table 1. On the other hand, there can also be a strong cooperation of the short-range forces to produce long-range order as typical of multidimensional polymorphism. The Cu sites in Cu_2O, for example, offer one of many crystal structures for which one or both of the ionic sites belong to a lower symmetry system than the crystal itself. This relates to the thermal relaxation phenomena that has taken place. Both long- and short-range effects are created within the matrix by the intrinsic properties and concentrations of the proximate cations and anions.

Packing and steric effects. The change in

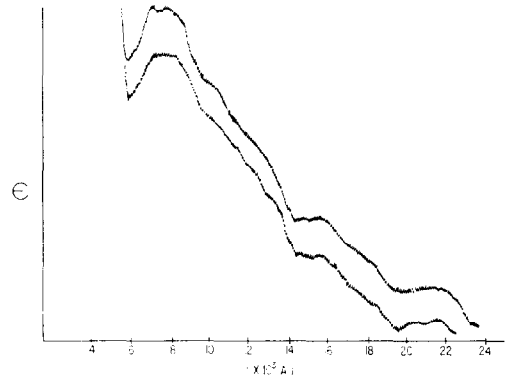

FIG. 6. Reflectance spectra of α-alumina containing 4.1% $CuCl_2$ and 1.08% $MgCl_2$.

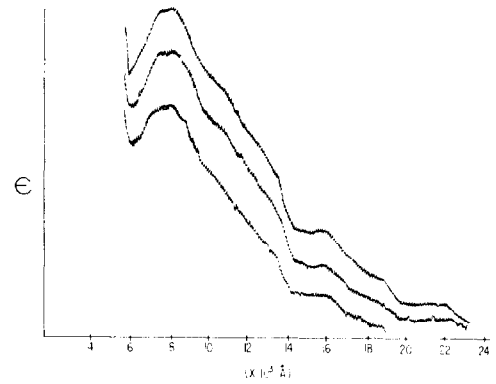

FIG. 8. Reflectance spectra of α-alumina containing 4% $CuCl_2$ and 0.95% LiCl.

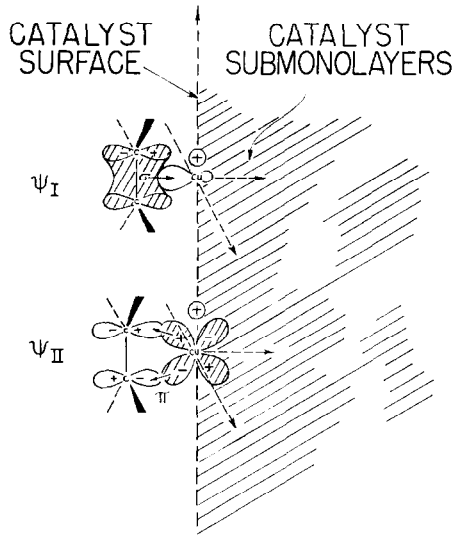

FIG. 9. Molecular orbitals for metal-olefin bonding. Ψ_I represents a σ type orbital symmetry, and Ψ_{II} a π type orbital symmetry in the complex. The shaded areas represent occupied orbitals and the unshaded areas indicate the unoccupied orbitals of the free metal ion and 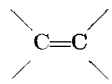 olefinic ligand.

the first coordination sphere of the atoms about the Cu(II)–Cu(I) site in the presence of Cs^+ and K^+ as opposed to the other alkali, alkaline earth, and lanthanide ions is brought about during the thermal transformation cycle by means of a *differential dilation* of the entire crystal structure after the point defect relaxation progresses throughout in each case and remains static after cooling. This phenomenon is common in simple structures of the CsCl and NH_4Cl type (*16*). Since octahedral voids are much larger than the tetrahedral voids in a close packing structure, the actual crystal structure of a particular atom can best fit into one or the other kind of void depending on its size relative to the void volume (*17*). Thus, the radius ratio* of an atom imposes a limitation on its coordination number. Both radius ratio and coordination number of the given ion are explicit functions of the relative ion polarizing strengths in the close packing model.

* The ratio of the radius of the central atom to that of the atoms coordinating it is referred to as the "radius ratio."

INTERACTIONS

The presence of cuprous chloride within the catalyst matrix decreases the induction period for the overall reaction because of its more effective complexation with ethylene and the rest of the unsaturated species present, as shown pictorially in Fig. 9. When present, the cuprous–cupric chloride couple is therefore much faster-acting than the cupric chloride alone. The rate of formation of cuprous chloride from cupric chloride is enhanced by higher operating temperatures, where the cuprous state of copper becomes more important than the cupric.

Since olefins form no strong complexes with the usual acceptor molecules, they are considered to be extremely poor Lewis bases, and so the concepts of bonding-synergism are employed to explain their behavior. Only a limited number of transition-metal ions can form olefin and acetylene complexes. The most common d^{10} ions involved are Cu^+, Ag^+, Hg^{2+}, and Pt^0, although Pt^{2+} must be included even though it is a d^8 ion. The olefins can act as monodentate or bidentate ligands with Cu^+ at the catalyst surface. In most cases, the copper ions assume a pseudotetrahedral or D_{2d} symmetry for best coordination wherein the olefinic, 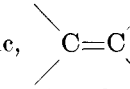 , system is essentially coplanar with the adjacent Cl atoms about the Cu^+ ion. This effect is observed in the X-ray studies of many other stable Cu^+ compounds (*18*).

Univalent copper and silver compounds exhibit many chemical similarities. The lower stability associated with Cu^+ and Ag^+ olefin complexes is due mainly to the low energy of the metal donar $3d$ orbitals and the increased availability of their $4p$ orbitals as shown in Fig. 9. The fact that the d^{10} ions are among the best coordinating agents known for olefins indicates that empty d^{10-n} orbitals are neither required nor essential for this type of organometallic bond formation. In order to form stable

TABLE 2
SPECTRAL BAND ASSIGNMENTS FOR COPPER(II) IN THE α-ALUMINA CATALYST MATRIX

Salts implanted in the catalyst	Transitions	Energy & average local Cu^{2+} ion site symmetry	
3.3% $CuCl_2$, 1.37% KCl	$^2B_2 \rightarrow {}^2A_1$	11,429 cm^{-1}	D_{2d}
0.6% $LaCl_3$ (Fig. 2)	$^2B_2 \rightarrow {}^2E_1$	9,707 cm^{-1}	
4% $CuCl_2$, 1.67% KCl	$^2B_2 \rightarrow {}^2A_1$	11,890 cm^{-1}	D_{2d}
(Fig. 3)	$^2B_2 \rightarrow {}^2E_1$	9,852 cm^{-1}	
3.9% $CuCl_2$, 4.1% CsCl	$^2E \rightarrow {}^2B$	10,989 cm^{-1}	D_{2d}
(Fig. 4)	$^2E \rightarrow {}^2A_1$	7,937 cm^{-1}	
4.1% $CuCl_2$, 1.08% $MgCl_2$	$^2T_{2g} \rightarrow {}^2E_g$	12,903 cm^{-1} ($10D_q$)	$\tilde{O}_h$
(Fig. 6)		8,403 cm^{-1}	
4.1% $CuCl_2$, 1.86% $LaCl_3$	$^2T_{2g} \rightarrow {}^2E_g$	12,346 cm^{-1}	$\tilde{O}_h$
(Fig. 7)		8,058 cm^{-1}	
4.0% $CuCl_2$, 0.95% LiCl	$^2T_{2g} \rightarrow {}^2E_g$	12,980 cm^{-1}	$\tilde{O}_h$
(Fig. 8)		8,003 cm^{-1}	

compounds and transition state intermediates the metal ion must be able to donate d electrons back into the anti-bonding p orbitals of the ligand, in this case the olefin. At the catalyst surface, charge must be transferred from olefin σ orbitals into the metal $4p$ orbitals, Ψ_I, while charge is being back-donated from the $d_{xz,yz}$ orbital set on the metal, Ψ_{II}, into the anti-bonding p orbitals of the olefin; thereby affecting a facile transfer of charge and subsequent bonding at the catalyst surface.

CONCLUSIONS

In each case, only the presence of K^+ and Cs^+ ions in the alumina matrix led to a D_{2d} symmetry field about the copper(II) ion point defects, whereby the transition metal is associated with four nearest neighbors. Therefore, we observe that highly polarizing cations generate octahedral voids and the low polarizing cations produce pseudotetrahedral voids during thermal transformations in the close packing model. This latter D_{2d} type of coordination is generated mainly by the short-range interactions and provides accessible chains of polarizable Cl^- ions of infinite length and high thermal stability lying in nearly the same plane. The discrete tetra halo complex ions, MCl_4^{2-}, can form whenever long-range electrostatic conditions permit the short-range isopolarization conditions to become established throughout the catalyst matrix.

The present work has emphasized the relative stability dependence of ionic solids on point-defect relaxation, symmetry, nearness, number, and polarizability of the charged ions involved in a given matrix under molten conditions. The studies also demonstrate clearly that the principal forces keeping copper(II) D_{2d} structures from becoming coplanar in these systems, i.e., D_{4h} or O_h, under isopolar conditions are mutual short-range repulsions of negative charges on the chloride ions dominant during the thermal cycle at each $CuCl_4^{2-}$ anion point defect site. The presence of the D_{2d} symmetry $CuCl_4^{2-}$ structure reduces the tendency for catalyst agglomeration and the subsequent correspondingly reduced reaction rates.

ACKNOWLEDGMENTS

I am indebted to the Diamond Shamrock Corporation Research Department, and extend special thanks to Dr. Carl Vinson for consultation and technical support; also to Dr. John P. Fackler, Jr., of Case Western Research University for the use of their facilities during the course of the work.

REFERENCES

1. DIMITROV, C., AND LEACH, H. F., *J. Catal.* **14**, 336 (1969); SPECTOR, M. L., HEINEMANN, H., AND MILLER, K. D., *Ind. Eng. Chem., Proc-*

cess Des. Develop. **6**(3), 327 (1967); HEINEMANN, H., *Chem. Tech.* **1**, 286 (1971); U. S. Patent 3,670,37; Japanese Patents 18331/66; 1968-4323; Canadian Patent 931,585.

2. PRETTRE, M., "Catalysis and Catalysts," Dover Publications, Inc., New York (1963); ANDERSON, R. B. (Ed.), "Experimental Methods in Catalytic Research," Academic Press, New York (1968); CAPRARA, G., MONTORS, G., AND LOVETERE, G., *Chimica e L'Industria (Milan)* **50**(2), 200-5 (1968).

3. CARRUBBA, R. V., AND SPENCER, J. L., *Ind. Eng. Chem. Process, Res. Develop.* **9**(3), 414-19 (1970).

4. BALLHAUSEN, C. J., "Introduction to Ligand Field Theory," McGraw-Hill Book Company, New York (1962); FIGGIS, B. N., "Introduction to Ligand Fields," Interscience Publishers, John Wiley and Sons, New York (1966); JØRGENSEN, C. K., "Absorption Spectra and Chemical Bonding in Complexes." Pergamon Press, New York (1962); ANDERSON, J. H., JR., *J. Catal.* **28**, 76 (1973).

5. WELLS, A. F., "Structural Inorganic Chemistry," Oxford University Press, London (1950); STOUT, G. H., AND JENSEN, L. H., "X-ray Structure Determination," The MacMillan Company, New York (1968); SMITH, J. V., AND BEWARD, A. S., "Powder Diffraction File," American Society for Testing and Materials STP 48-M2 (1963); "Powder Diffraction File 1972," JCPDS, 18-349, 1601 Park Lane, Swarthmore, Pennsylvania, 1972.

6. SUGANO, S., TANABE, Y., AND KAMIMURA, H., "Multiplets of Transition-Metal Ions in Crystals," Academic Press, New York (1970); LEVER, A. B. P., "Inorganic Electronic Spectroscopy," American Elsevier, New York (1968); WELLS, A. F., *J. Chem. Soc. (London)* **1662** (1947); HELMHOLZ, L., AND KRUH, R. F., *J. Am. Chem. Soc.* **74**, 1176 (1952); MOROSIN, B., AND LINGAFELTER, E. C., *J. Phys. Chem.* **65**, 50 (1961); DOTSON, R. L., *J. Inorg. Nucl. Chem.* **34**, 3131 (1972); MCGINNETY, J. A., *J. Amer. Chem. Soc.* **94**, 8406 (1972).

7. ENGLMAN, R., "The Jahn-Teller Effect in Molecules and Crystals," Wiley-Interscience, John Wiley and Sons, Inc., New York (1972).

8. KUNII, D., AND LEVENSPEIL, O., "Fluidization Engineering," John Wiley & Sons, Inc. (1962); LIPSETT, S. G., JOHNSON, F. M. G., AND MAASS, O., *J. Am. Chem. Soc.* **49**, 925, 1940 (1927); **50**, 2701 (1928); BENSON, G. C., AND BENSON, G. W., *Rev. Sci. Instr.* **26**, 477 (1955).

9. BRAUNSTEIN, J., MAMANTOV, G., AND SMITH, G. P., "Advances in Molten Salt Chemistry," Vol. 1, Plenum Press, New York, N. Y., 1971; BLANDER, M., "Molten Salt Chemistry," Interscience Publishers, John Wiley and Sons, New York, 1964.

10. ADAMSON, A. W., "Physical Chemistry of Surfaces," Interscience Publishers, New York, 1967.

11. Canadian Patent #932,341.

12. TEMKIN, M., *Acta Physicochim. URSS* **20**, 411 (1945).

13. PELTON, A. D., AND THOMPSON, W. T., *Can. J. Chem.* **48**, 1585 (1970); LUMSDEN, J., "Thermodynamics of Molten Salt Mixtures," Academic Press, New York, N. Y. (1966), pp. 245–250; DELIMARSKII, IU. K., AND MARKOV, B. F., "Electrochemistry of Fused Salts," Medical and Technical Summaries, Inc., 2419 M. St., N.W., Washington, D. C.

14. FELSENFELD, G., *Proc. Roy. Soc. (London)*, A236 **506** (1956).

15. PELTON, A. D., *Can. J. Chem.* **49**, 3919 (1971); PAPATHEODOROU, G. N., *J. Inorg. Nucl. Chem.* **35**, 465 (1973); RICH, R. L., "Periodic Correlations," W. A. Benjamin, Inc., New York (1965); BRIANT, C. L., AND BURTON, J. J., *Nature* **243**(128), 100–102 (1973).

16. VERMA, A. R., AND KRISHNA, P., "Polymorphism and Polytypism in Crystals," John Wiley and Sons, Inc., New York, 1966; NOWICK, A. S., AND BERRY, B. S., "Anelastic Relaxation in Crystalline Solids," Academic Press, New York, 1972.

17. WELLS, A. F., *J. Solid State Chem.* **6**, 469–478 (1973).

18. COATES, G. E., AND WADE, K., "Organo-Metallic Compounds," Vol. I, Methuen and Co., Ltd., London (1967); GREEN, M. L., "Organo-Metallic Compounds," Vol. II, Methuen and Co., Ltd., London (1968); FISHER, E. O., AND WERNER, H., "Metal Pi-Complexes, Vol. 1: Complexes with Di- and Oligo-Olefinic Ligands," American Elsevier Pub. Co., New York (1966); CUMPER, C. W. N., "Wave Mechanics for Chemists," Heinemann, London (1966).